Journal of Theoretical and Applied Information Technology
15th March 2024. Vol.102. No 5

ISSN: 1992-8645 www.jatit.org E-ISSN: 1817-3195

A FUSED 3D-2D CONVOLUTION NEURAL NETWORK FOR SPATIAL-SPECTRAL FEATURE LEARNING AND HYPERSPECTRAL IMAGE CLASSIFICATION

MURALI KANTHI[1], J. DAVID SUKEERTHI KUMAR[2], K. VENKATESHWARA RAO[3], MOHMAD AHMED ALI[4], SUDHA PAVANI K[5], NUTHANAKANTI BHASKAR[6], T. HITENDRA SARMA[7]

[1,5]Department of Computer Science & Engineering (Data Science), CMR Technical Campus, Hyderabad, India.
[2]Department of Computer Science & Engineering, Santhiram Engineering College, Nandyal, Andhra Pradesh, India.
[3]Department of Computer Science & Engineering, CMR College of Engineering & Technology, Hyderabad, India.
[4]Department of Computer Science & Engineering, CMR Institute of Technology, Hyderabad, India.
[6]Department of Computer Science & Engineering, CMR Technical Campus, Hyderabad, India.
[7]Department of Information Technology, Vasavi College of Engineering, Hyderabad, India.
E-mail: [1]murali.kanthi@gmail.com, [2]jdsk22@gmail.com, [3]vrkatevarapu@gmail.com,
[4]ahmedmca2004@gmail.com, [5]sudhapavani1@gmail.com, [6]bhaskar4n@gmail.com,
[7]t.hitendrasarma@gmail.com

ABSTRACT

Hyperspectral image (HSI) classification is a prominent topic in the area of remote sensing and it is challenging task since the minimal number of labelled training samples and the high dimensional space that includes a wide range of spectral bands. Therefore, a more effective neural network architecture needs to be created to boost the effectiveness of the HSI classification job. To tackle these issues, we present an innovative fused 3D-2D convolutional neural network (F-CNN), that extracts both spectral-spatial features and enhances the HSI classification efficiency by incorporating three fusion blocks sequentially into the proposed model. Each fusion block includes a module of 3D-2D CNNs to retrieve and fuse the spectral-spatial information for the improvement of HSI classification task. Three standard datasets that are freely available (Salinas, Pavia University, and Indian Pines) and new Indian datasets (Ahmedabad-1 and Ahmedabad-2) are carried out in experimental investigation to determine the efficiency of the presented model. The proposed F-CNN model has achieved accuracies of 80.79% on the AH1 (Ahmedabad-1) dataset, 87.98% on the AH2 (Ahmedabad-2) dataset, 99.99% on the PU (Pavia University), 99.99% on the SA (Salinas), and 99.92% on the IP (Indian Pines) dataset. According to research findings, the provided model outperforms the remaining current techniques in terms of classification performance.
Keywords: *Hyperspectral Image, Deep Learning, Convolutional Neural Network, Classification, Spectral-Spatial Information*

1. INTRODUCTION

In recent years, it has become relatively simple to acquire hyperspectral remote sensing images with highest spatial-spectral resolution. Since hyperspectral images are so effective in resolving fine spectra, they can be used in a variety of applications, including military, environmental, mining, and medical fields [1]. A well-known study in the field of remote sensing is the classification of hyperspectral images (HSI), which is a difficult issue because there aren't many labelled training samples and a lot of spectral bands in the high-dimensional space. Because they can account for the substantial spectrum information acquired in hyperspectral pictures, traditional image classification techniques like KNN and SVM classifiers have done well for this challenge [2]. The studies [3-5] provide in-depth reviews of this research. Due to the tremendous success of deep learning, convolutional neural

network (CNN)-based algorithms have lately achieved excellent results for a variety of image analysis-related tasks, including object identification and image categorization.

Deep CNN methods have been shown to be efficient at retrieving features, resulting to an increase in the classification accuracy of HSI [6]. To attain a high level of classification precision, it is essential to get spatial-spectral features with high discrimination [7-8]. When classifying hyperspectral images, it is important to take the spectral-spatial perspectives into account. A hyperspectral image, often referred to as a spectral perspective image, is essentially composed of several smaller "images," each of which denotes a certain wavelength band of the electromagnetic spectrum. As a result, hyperspectral images are often represented using 3D spectral-spatial data. Hyperspectral photos record objects from a variety of angles, but current CNN-based approaches [9–11] that solely take into account spatial or spectral information are forced to disregard the interconnectedness of the two. Essentially, the interconnected data can be used to improve categorization success. As a result, a somewhat decent CNN-based classifier can be trained with just a few labelled 3D spectral-spatial images.

The simultaneous modeling of spectral and spatial information has been the subject of a number of early attempts [12–14]. These techniques, also known as 3D-CNN models, use arrayed convolution operations on spectral-spatial feature regions in a layer-by-layer manner. The generated feature maps show how this particular 3D-CNN method is advantageous. The main disadvantage of these methods is that creating a deep 3D-CNN method is hard since more training examples are required because the public HSI datasets are so small.

We proposed the Fused-CNN (F-CNN) model for HSI classification. In the presented F-CNN, the 3D-CNN module and the 2D-CNN module are combined collectively. Therefore, as seen in Fig. 1, the proposed F-CNN incorporates 2D-CNNs with 3D-CNNs to acquire the significant characteristics, as opposed to traditional 3D-CNNs which build 3D convolution layer by layer. After that, a concatenation model is utilized to merge the 2D and 3D features. Experimental results on a benchmark dataset have demonstrated that the new F-CNN outperforms a number of cutting-edge HSI classifiers. The following enumerates the work's efforts:

- The proposed a novel F-CNN model which incorporates 3D-CNN with 2D-CNN to gather the important characteristics from HSI and improve the accuracy of classification.
- The designated F-CNN superiors other modern HSI classifiers, according to substantial investigations on freely accessible datasets, which have produced positive results.

The rest of the work is arranged this way: Section 2 presents the literature review for the proposed work, while Section 3 presents the model architecture. The results of the established method's experimental research are presented in Section 4. The conclusions are presented in Section 5 to close.

2. LITERATURE REVIEW

The research community as a whole agrees that a major challenge in the discipline is the classification of hyperspectral images. Nonetheless, the majority of the research done before now used conventional computational methods. In this section, we provide a brief overview of the most recent deep learning-based models, which are primarily separated into 2D-CNN and 3D-CNN models for the sake of this study.

2.1 2D-CNN Based Models

2D-CNN architectures are often employed to evaluate spatial-spectral information separately from the primary HSI dataset by minimizing the spectral scale with a dimensionality reduction approach like principal component analysis and reducing spatial regions of pixel-cantered neighbors. To recover the spectral-spatial information encoded in HSIs, [15-18] introduced a 2D-CNN technique, which has been utilized to analyze the band selection results supplied by Ada-Boost-SVM. In order to classify HSI using the band-selection results, many methods were proposed to combine distinct 2D-CNN models. To obtain in-depth spectrum features, for instance, Li et al. [19] employed deep belief networks. To classify the HSIs, Sarma et al. [20] presented a deep channel responsive convolutional network with two sub-sections. One section for pull out the spectral characteristics, and another for combine the characteristics from various channels. For the purpose of performing band-selection for HSIs, Lorenzo et al. presented an attention-based CNN in [21].

Additionally, A semi-supervised 2D-CNN method containing the encoder, distorted encoder, and decoder components was also presented by Liu et al. [9]. The classification model is tuned to reduce the restoration omission within both the input images and the combination of labelled and unlabeled images. To incorporate the underlying information of each input sequence in an adaptive fashion, Zhu et al. [22] introduced a 2D-CNN adaptive HSI classification network made up of flexible convolutions and down sampling. Yue proposed a 2D-CNN approach to evaluate spectral-spatial qualities by augmenting spatial regions with three feature regions based on spectrum information (see [23]). A spectral-spatial feature-based categorization approach, such as the one described by Zhao and Du [24], collects spatial data with the help of a 2D-CNN and locates spectral data with the help of a linear local distinction model. While these techniques may theoretically provide comparably performing models, the large training datasets they necessitated made them impractical for most real-world applications.

2.2 3D-CNN Based Models

There are methods that take into consideration the HSI data's spectral and geographical characteristics. CNN models' adaptability allows for the development of numerous approaches and networks for spectral-spatial analysis. When it comes to extracting spectral-spatial properties for classification, Yushi et al. [25] presented a deep 3D-CNN approach using several 3D convolution layers. A deep model that also relies heavily on spatial information was given by Lee [26]. Li et al. [17] suggested a 3D-CNN approach that layered 3D convolution layers instead of the pool layer, in contrast to [26]. The suggested model can faithfully reproduce the changes in regional impulses as reported by the spectral-spatial data. A. Ben et al. [27] developed and evaluated a pair of 3D patterns that integrate the typical 3D convolution processes to let a coordinated spatial-spectrum information inspection, with the goal of evaluating a series of volumetric methods of the HSI.

Nonetheless, some hybrid methods combined 2D-CNNs and 3D-CNNs. One such model is HybridSN, proposed by Roy et al. [28], which combines spectrum and spatial 3D-CNN with spatial 2D-CNN. P. Babu et al. [29] established stratified image synthesis network for HSI classification to combine groupings of images based on shared spectral properties. For HSI classification, C. Gong et al. [30] presented a multiscale graph convolution network for convolution in irregular picture regions. In order to develop a dense multiscale hybrid network and a multi-scale HSI spatial and spectrum representation, Li et al. [31] used feed-forward connections as shortcuts to reach all convolutional layers' hierarchical input. Mohan et al. [32] introduced HybridCNN for use in Classification problems. In order to obtain information from the spatial and spectrum bands, Kanthi et al. [33] presented a deep CNN method that makes use of three separate multi-scale spatial-spectrum areas. Murali et al. [28] introduced a 3D-CNN technique for classifying HSI using deep spectral-spatial data by partitioning HSI into 3D regions.

In comparison to 2D-CNN-based approaches, 3D-CNN-based methods definitely have more characteristics. Therefore, the network complexity and memory needs of the 3D-CNN-based models are much larger than those of the 2D-CNN-based approaches. It appears that these 3D-CNN-based methodologies cannot be directly applied to modelling such entangled interactions because of the following. Due to the prevalence of multi-layer 3D convolutional networks in current 3D-CNN-based methods, optimizing the prediction loss via these nonlinear designs is a significant challenge. This study advocated fusing the features acquired from 2D-3D convolution actions in progressive way and simultaneously developing a mixed 3D-2D CNN model with comparatively few training instances to gain from both the benefits of the 3D and 2D CNN based techniques.

3. METHOD

In this part, we provide the presented fused 3D-2D CNN (F-CNN) method elaborately. As seen in Fig. 1, the developed model F-CNN uses input from both 3D and 2D patches to generate fused spatial-spectral deep features from the HSI. Consider the input HSI to be a 3D cube, with sides of length W, height H, and height B, wherein W and H represent the horizontal and vertical dimensions of the image, respectively, and B is the number of spectral channels.

In an effort to reduce the number of channels, principal component analysis (PCA) was used; ultimately, 30 spectrum bands are selected for the IP dataset, and 15 spectrum bands are selected for the other datasets included in the study; this is in line with the most popular existing architectures for CNN [34-39]. In the presented 3D-2D CNN (F-CNN) network, we established three F-CNN blocks one after another to retrieve deep spatial-spectral

characteristics from the HSI data to enhance the hyperspectral image classification performance. In this approach, 3D-CNN and 2D-CNN networks are trained parallelly in every F-CNN block to extract more discriminative features. In the first F-CNN block, 3D and 2D image patches are given to 3D-CNN model and 2D-CNN model as input. Each 3D and 2D patches have the dimensions w x h x d, w x h respectively, where w_i, h_i denotes the i patch's width and height, d its depth. All of the investigations in this study make use of Google's Colab Pro GPU, which has RAM of 25.51 GB. In light of this setup, we have selected intuitive 3D and 2D patches with sizes of w x h x d = 25 x 25 x 30 and w x h = 25 x 25. As presented in Fig. 1, in every block, 3D-CNN and 2D-CNN models contain two convolution layers ($Conv_1$ and $Conv_2$), max pooling layer ($Pool$) and two sets of filters $K_1 = 16$ and $K_2 = 32$ with size 3 x 3 x 7 *and* 3 x 3 x 5 respectively for 3D-CNN model and 3 x 3 and 3 x 3 respectively for the 2D-CNN model. In both the models, batch normalisation layer and activation function ReLU is employed after every convolution layer. The max-pool layer with strides 2 x 2 and 2 x 2 x 2 respectively are applied for both the models after the first convolutional layer as Eq. (1).

$$f(i) = \begin{cases} 0, & i < 0 \\ i, & i \geq 0 \end{cases} \quad (1)$$

The features retrieved from both the 3D-CNN and 2D-CNN networks in the F-CNN block-I are provided to concatenation layer ($Conc_1$) to merge the retrieved characteristics to given to F-CNN block-II. In the F-CNN block-II, the generated ($Conc_1$) feature map is employed as input and fed to the same 3D and 2D F-CNN networks for additional feature extraction. The concatenation ($Conc_2$) layer, like block-I, receives the features extracted from these two networks and feeds them to block-III of the F-CNN. In block III, the same procedure is performed using the ($Conc_2$) feature map to build the ($Conc_3$) feature map, which is employed to retrieve further discriminative context characteristics.

The extracted feature map ($Conc_3$) from block-III is flattened and sent to the fully connected layers fcl_1, fcl_2, and fcl_3 for classification. every neuron's activity function is determined using Eq. (2).

$$Actv_i(fcls = r(w_i(fcls) * actv_{i-1}(fcls) + b_i) \quad (2)$$

Where b_i is the bias and $w_i(fcsl)$ is the weighted aggregate of each earlier layer input. The ReLU activation is denoted by $r(.)$.

A soft-max probability model classifies the data last. $F = [F_i]i$, wherein i is a positive number ranging from one and m, provides the representation of features once the model is executed as (3).

$$\text{Smax}(F)_i = \frac{e^{F_i}}{\sum_{i=1}^{k} e^{F_j}} \text{ for } i = 1, 2, .., m \quad (3)$$

The last function is argmax. It locates a function's highest relevant characteristics. Equation (3) assigns classes to m HSI class-labels from $U = \{1,2,3,4,,,\text{m}\}$.

Table 1. Benchmark and Indian HSI datasets-Description.

Parameters	AH-1	AH-2	SA	PU	IP
Sensor	AVIRIS-NG	AVIRIS-NG	AVIRIS	ROSIS	AVIRIS
Wavelength Range	0.37–2.5µm	0.37–2.48 µm	360–2500 µm	0.43–0.86 µm	0.4–2.5µm
No. of Classes	5	7	16	9	16
No. of Spectral Bands	351	370	200	115	200
Spatial Dimension	300 × 200	300 × 200	512 × 217	610 × 340	145 ×145

Journal of Theoretical and Applied Information Technology
15th March 2024. Vol.102. No 5

ISSN: 1992-8645 www.jatit.org E-ISSN: 1817-3195

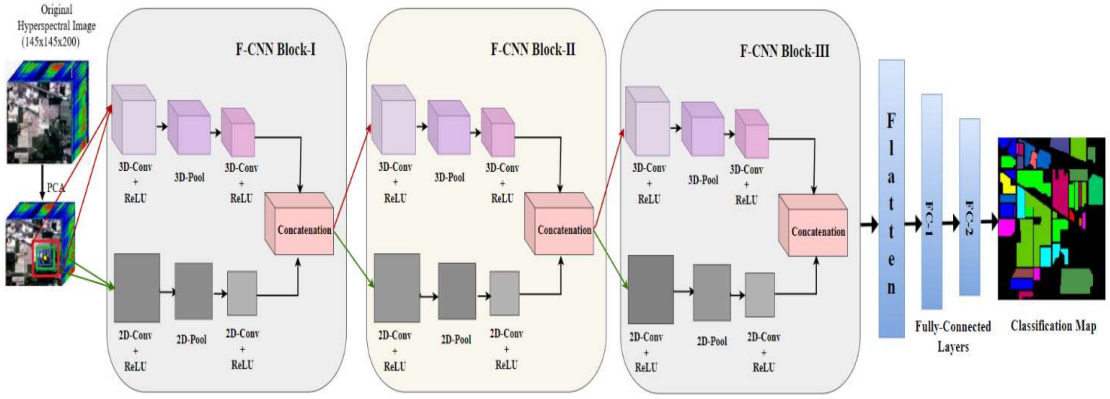

Figure. 1: Overview of the presented Fused 3D-2D CNN (F-CNN) network.

Table 2. Benchmark Datasets- Classification Accuracies.

Model	SA			PU			IP		
	AA	OA	Kappa	AA	OA	Kappa	AA	OA	Kappa
2DCNN	94.64	94.95	94.24	92.87	93.19	92.04	88.28	91.68	90.64
3DCNN	97.08	96.97	96.37	96.15	96.56	95.54	94.57	95.15	93.97
Hybrid-SN	99.58	99.86	99.51	99.04	99.92	99.82	98.57	99.23	99.13
Hybrid-CNN	100	100	100	99.98	99.99	99.99	99.72	99.80	99.76
MS3DCNN	100	100	100	99.97	99.99	99.99	98.87	99.89	99.24
Proposed Method	100	100	100	99.99	99.99	99.99	98.96	99.92	99.82

Table 3. Proposed Model Classification Accuracies with Few Training Data.

Dataset	5 % Training Samples			10% Training Samples		
	AA	OA	Kappa	AA	OA	Kappa
IP	96.31	95.42	95.21	98.68	99.12	98.46
PU	97.87	98.45	97.83	98.75	99.54	98.82
SA	98.72	98.76	98.57	98.59	99.12	98.73
AH-1	80.25	80.74	78.12	82.41	82.76	81.25
AH-2	72.86	72.89	71.46	75.42	75.98	73.81

Table 4. Indian Datasets-Classification Accuracies.

Model	AH-1			AH-2		
	AA	OA	Kappa	AA	OA	Kappa
3DCNN	82.42	80.98	78.18	69.31	70.07	67.94
Hybrid-SN	85.04	85.68	83.77	76.72	79.56	75.83
Hybrid-CNN	84.98	85.45	83.46	76.25	78.23	74.43
MS3DCNN	87.16	87.25	85.75	77.06	80.11	76.73
Proposed Method	87.86	87.98	85.76	77.82	80.79	76.99

4. RESULTS AND DISCUSSION

In this section, the F-CNN model's experimental setups, dataset descriptions, and experimental evaluation are all shown. The following subsections provide more information.

4.1 Description of Datasets and Experimental Setup

Three freely available HSI datasets, SA (Salinas), PU (Pavia-University), and IP (Indian-Pines), were used in an experimental analysis. For the IP dataset, which was obtained from the Indian-Pines test site in northwest Indiana, 16 class-labels are given as the ground truth. With the use of nine ground-truth class labels, PU was captured during a flying campaign over Pavia, northern Italy. 16 class labels from the Salinas Valley were used to gather the ground truth for the SA. Additionally, two brand-new Indian datasets, AH1 (Ahmedabad-1) and AH2 (Ahmedabad-2), were used to test the effectiveness of the performance of the method that was provided. The ISRO collected these datasets using the AVIRIS-NG sensor [39]. Table 1 provides the specifics.

The Google Cloud is used to run the experiments on a GPU with 25 GB of RAM. Twenty percent of data is used for training the established network F-CNN, while the remaining eighty percent is used for testing. The Adagard optimizer is used, together with a decaying (1e-06) and learning-rate-constrained (0.001) categorical cross-entropy. The method was trained with a 32-batch size across 50 epochs. The trials were repeated 15 times on each dataset, and the mean results were recorded.

4.2 Analysis of Classification Results

Standard metrics like AA (Average-Accuracy), K (Kappa), and OA (Overall-Accuracy) were added to evaluate the quality of the offered system. The findings of the presented F-CNN model are compared to those of other modern HSI classification methods such as 3DCNN [33], 2DCNN [5], Hybrid-SN [28], Hybrid-CNN [32], and MS3DCNN [35]. Table 2 shows the classification accuracy achieved by each of these methods. The results show that the provided model obtained a perfect OA and AA score on Salinas, a 99.99% OA and AA score on Pavia, and a 99.92% OA and 98.96% AA score on IP. Table 2 shows that the classification effectiveness of the presented method is higher than that of alternative models on the contrast datasets, as measured by K, AA, and OA. The results for the 2DCNN, 3DCNN, Hybrid-SN, Hybrid-CNN, and MS3DCNN models' accuracies are collected from their corresponding articles, and the code for the similar models is available to the public. The provided model has significantly higher kappa, AA, and OA values than the current gold standard. The provided method outperforms the HybridSN strategy in nearly all cases. In addition, while the HybridSN model trained on 30% of examples, the presented technique uses 20% of samples, selected at random from each category. Table 3 indicates the efficiency of the presented approach based on the amount of the training data. The given model outperformed state-of-the-art approaches in classification efficacy with less training data.

This is being done by conducting tests on two new Indian datasets (AH1 and AH2) to guarantee the method's efficacy and robustness. We compared our method against others using freely available code, including 3D-CNN, HybridSN, HybridCNN, and MS-3DCNN. The code was not made available; therefore, it could not be compared to other approaches. On the AH1 dataset, the suggested technique attained 87.98% OA and 87.86% AA, whereas on the AH2 dataset, it attained 80.79% OA and 77.82% AA. Table 4 displays the results of using the specified model on the updated datasets. Figure 2 depicts a comparison of the accuracy of the proposed model to that of existing approaches on the benchmark datasets and the Indian datasets.

The accuracy and loss progress of the presented technique throughout 100 epochs of validation and training samples are presented in Fig. 3. The method's rapid convergence could be identified in fact that the progress occurs in roughly 50 epochs. Figures 4 through Figure 8 show the classification maps that the proposed model produced for each dataset. Classification maps generated by the proposed method are more easily comparable to those generated by competing methods. The proposed model has less noise in some of its maps than others.

5. CONCLUSION

A novel F-CNN approach for HSI classification is advised in this paper, which retrieves both spatial-spectral features from the hyperspectral image and enhances the HSI classification performance by incorporating three fusion blocks sequentially into the proposed model. Each fusion block includes a module of 3D-2D CNNs to extract and fuse the spatial-spectral properties for the improvement of

HSI classification task. The presented approach outperforms current methods in terms of efficiency, according to experiments using benchmark datasets. The established approach is evaluated further on new datasets, and it is found to be more accurate than the Hybrid-SN and Hybrid-CNN models. On both the standard and Indian datasets, the proposed method improved accuracy by between one and two percent. The purpose of this study is to decrease the training time of each fusion block in the future, resulting in a reduction in the model's overall training time.

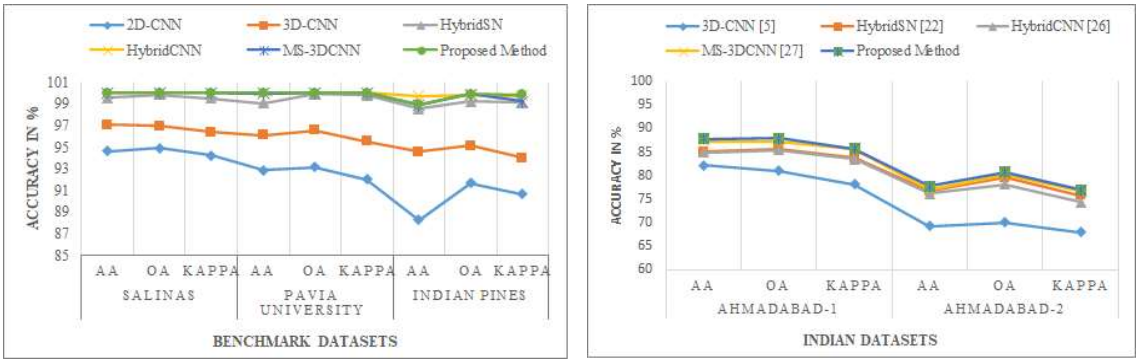

(a) (b)

Figure. 2. Proposed approach efficiency comparison with contemporary methods: (a) Standard datasets (b) Indian datasets.

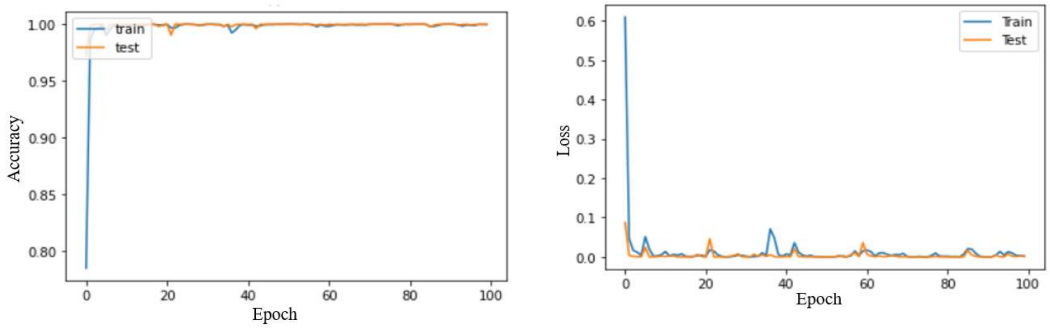

(a) (b)

Figure 3. Presented method's testing and training on Indian Pines: (a) Accuracy, (b) Loss.

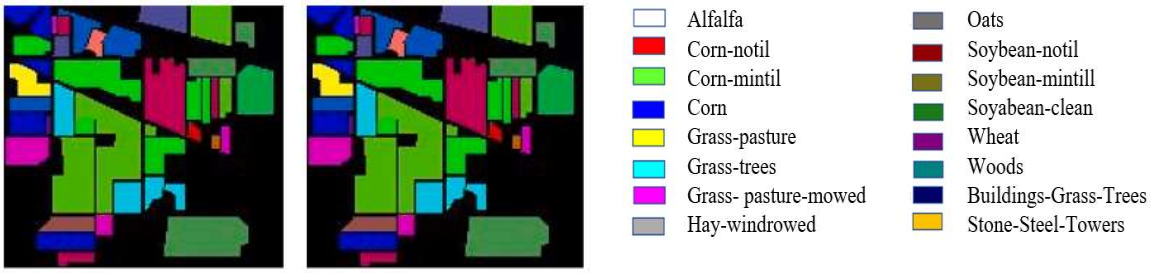

(a) (b) (c)

Figure. 4. IP (a) image-ground-truth, (b) classification map, (c) fables of class.

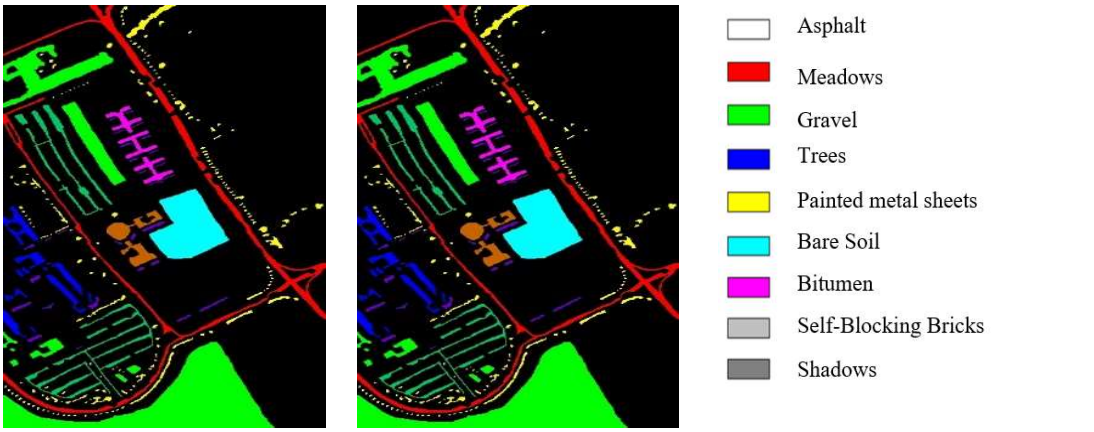

(a) (b) (c)

Figure. 5. PU (a) image-ground-truth, (b) classification map, (c) fables of class.

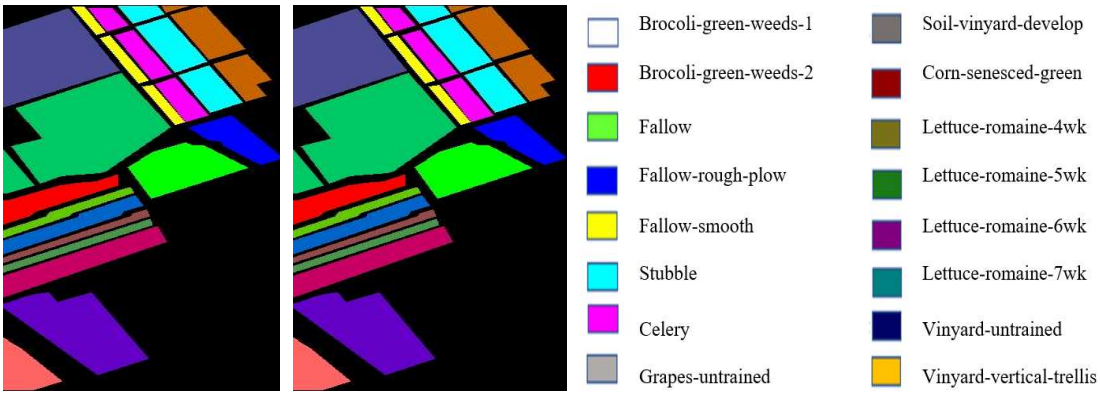

(a) (b) (c)

Figure. 6. SA (a) image-ground-truth, (b) classification map, (c) fables of class.

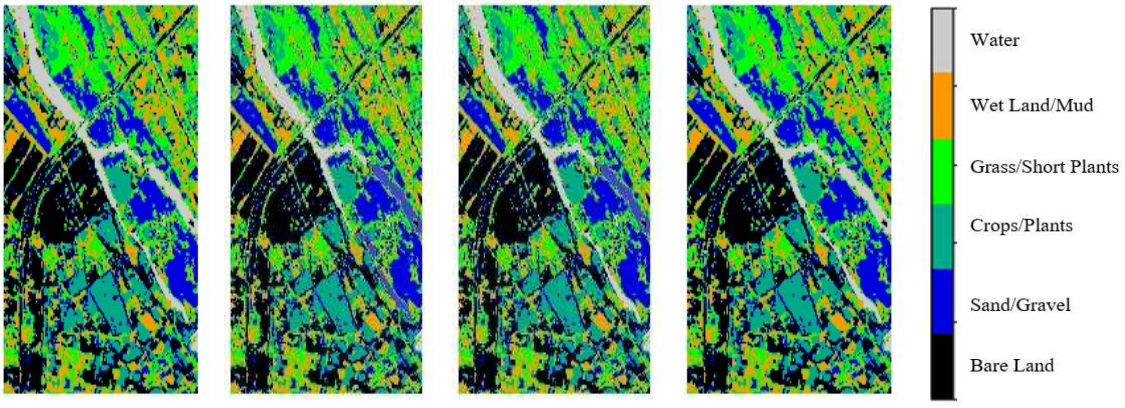

(a) (b) (c) (d)

Figure. 7. AH-1 (a) image-ground-truth, (b) Hybrid-SN map, (c) MS3DCNN map, (d) proposed model classification map with fables of class.

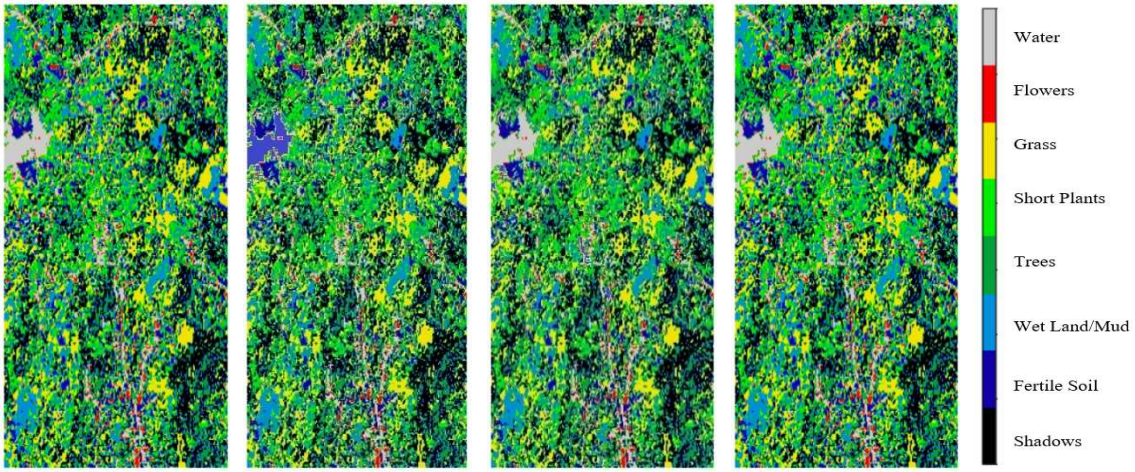

Figure. 8. AH-2 (a) image-ground-truth, (b) Hybrid-SN map, (c) MS3DCNN map, (d) proposed model classification map with fables of class..

REFERENCES:

[1] JM. Bioucas-Dias A. Plaza, G. Camps-Valls, P. Scheunders, NM. Nasrabadi, J. Chanussot, "Hyperspectral remote sensing data analysis and future challenges" *IEEE Geosci Remote Sens Mag.* 2013;1(2):6–36.

[2] A. Plaza, JA. Benediktsson, JW. Boardman, J. Brazile, L. Bruzzone, G. Camps-Valls, J. Chanussot, M. Fauvel, P. Gamba, A. Gualtieri, "Recent advances in techniques for hyperspectral image processing". *Remote Sens Environ.* 2009;113: S110–S122.

[3] I. B. Strachan, E. Pattey, and J. B. Boisvert, "Impact of nitrogen and environmental conditions on corn as detected by hyperspectral reflectance, "Remote Sensing of environment, vol. 80, no. 2, 2002, pp. 213–224.

[4] S. Jay and M. Guillaume, "A novel maximum likely hood-based method for mapping depth and water quality from hyperspectral remote sensing data," Remote Sensing of Environment, vol. 147, 2014, pp. 121–132.

[5] C. J˙anicke, A. Okujeni, S. Cooper, M. Clark, P. Hostert, and S. van derLinden, "Brightness gradient-corrected hyperspectral image mosaics for fractional vegetation cover mapping in northern california," *Remote Sensing Letters*, vol. 11, no. 1, 2020, pp. 1–10.

[6] X. Shang and L. A. Chisholm, "Classification of australian native forest species using hyperspectral remote sensing and machine learning classification algorithms," *IEEE Journal of Selected Topics in Applied Earth Observations and Remote Sensing,* vol. 7, no. 6, 2013, pp. 2481–2489.

[7] M. Kanthi1, TH. Sarma, CS. Bindu. "A Survey: Deep learning classifiers for hyperspectral image classification". *Journal of Theoretical and Applied Information Technology,* vol 99, no. 24, 2021, pp. 6042-6053.

[8] J. Peng, W. Sun, HC. Li, W. Li, X. Meng, C. Ge, Q. Du, "Low-rank and sparse representation for hyperspectral image processing: A review". *IEEE Geosci Remote Sens Mag,* vol. 10(1), 2022, pp. 10–43.

[9] W. Li, EW. Tramel, S. Prasad, JE. Fowler, "Nearest regularized subspace for hyperspectral classification". *IEEE Trans Geosci Remote Sens,* vol. 52(1), 2014, pp. 477–489.

[10] Kanthi, Murali, K. Venkateshwara Rao, L. Chandra Sekhar Reddy, T. Hitendra Sarma, Nuthanakanti Bhaskar, and Nam Vasundhara. "3D-CAN: A 3D Convolution Attention Network for Feature Extraction and Classification of Hyperspectral Images." *In 2023 International Conference on Network, Multimedia and Information Technology (NMITCON)*, pp. 1-6. IEEE, 2023.

[11] Kanthi, Murali, K. Venkateshwara Rao, Nuthanakanti Bhaskar, Shankar Nayak Bhukya, and T. Hitendra Sarma. "A Multiple Branch Fusion Network for Feature Learning and Hyperspectral Image Classification." *In 2023 14th International Conference on Computing*

Communication and Networking Technologies (ICCCNT), pp. 1-5. IEEE, 2023.

[12] Li, Xiaoxu, Z. Sun, JH. Xue, and Z. Ma. "A concise review of recent few-shot meta-learning methods.", *Neurocomputing*, vol. 456, 2021, pp. 463-468.

[13] Liu, Bing, X. Yu, A. Yu, P. Zhang, G. Wan, R. Wang. "Deep few-shot learning for hyperspectral image classification." *IEEE Transactions on Geoscience and Remote Sensing*, vol. 57(4), 2018, pp. 2290-2304.

[14] Gao, Hongmin, Y. Yang, C. Li, L. Gao, B. Zhang. "Multiscale residual network with mixed depthwise convolution for hyperspectral image classification.", *IEEE Transactions on Geoscience and Remote Sensing*, vol. 59(4), 2020, pp. 3396-3408.

[15] Jia, Sen, Z. Lin, M. Xu, Q. Huang, J. Zhou, X. Jia, Q. Li. "A lightweight convolutional neural network for hyperspectral image classification." *IEEE Transactions on Geoscience and Remote Sensing,* vol. 59, no. 5, 2020, pp. 4150-4163.

[16] Cui, Benlei, XM. Dong, Q. Zhan, J. Peng, W. Sun. "LiteDepthwiseNet: A lightweight network for hyperspectral image classification." *IEEE Transactions on Geoscience and Remote Sensing,* vol. 60, 2021, pp. 1-15.

[17] Li, Wei, C. Chen, M. Zhang, H. Li, Q. Du. "Data augmentation for hyperspectral image classification with deep CNN.", *IEEE Geoscience and Remote Sensing Letters*, vol. 16, no. 4, 2018, pp. 593-597.

[18] Haut, J. Mario, M. E. Paoletti, J. Plaza, A. Plaza, J. Li. "Hyperspectral image classification using random occlusion data augmentation.", *IEEE Geoscience and Remote Sensing Letters,* vol. 16, no. 11, 2019, pp. 1751-1755.

[19] X. Li, M. Ding, A. Pižurica, "Group convolutional neural networks for hyperspectral image classification". Paper presented at: *ICIP 2019. Proceedings of the IEEE International Conference on Image Processing (ICIP);* 2019 Sep 22–25; Taipei, Taiwan; p. 639–643.

[20] Sarma, Vivek, A. Diba, T. Tuytelaars, and L. V. Gool, "Hyperspectral CNN for image classification & band selection, with application to face recognition", *Technical report KUL/ESAT/PSI/1604, KU Leuven, ESAT, Leuven, Belgium*, 2016.

[21] Liu, Peng, H. Zhang, and K. B. Eom, "Active deep learning for classification of hyperspectral images.", *IEEE Journal of Selected Topics in Applied Earth Observations and Remote Sensing,* vol. 10, no. 2, 2016, pp. 712-724.

[22] Zhu, Jian, L. Fang, and P. Ghamisi, "Deformable convolutional neural networks for hyperspectral image classification.", *IEEE Geoscience and Remote Sensing Letters,* Vol. 15, No. 8, pp. 1254-1258, 2018.

[23] Yue, Jun, W. Zhao, S. Mao, and H. Liu, "Spectral–spatial classification of hyperspectral images using deep convolutional neural networks.", *Remote Sensing Letters*, Vol. 6, No. 6, pp. 468-477, 2015.

[24] Zhao, Wenzhi, and S. Du. "Spectral–spatial feature extraction for hyperspectral image classification: A dimension reduction and deep learning approach.", *IEEE Transactions on Geoscience and Remote Sensing*, Vol. 54, No. 8, pp. 4544-4554, 2016.

[25] Chen, Yushi, H. Jiang, C. Li, X. Jia, and P. Ghamisi, "Deep feature extraction and classification of hyperspectral images based on convolutional neural networks.", *IEEE Transactions on Geoscience and Remote Sensing*, Vol. 54, No. 10, pp. 6232-6251, 2016.

[26] Lee, Hyungtae, and H. Kwon, "Contextual deep CNN based hyperspectral classification.", *In 2016 IEEE international geoscience and remote sensing symposium (IGARSS)*, IEEE, pp. 3322-3325, 2016.

[27] Hamida, A. Ben, A. Benoit, P. Lambert, and C. B. Amar, "3-D deep learning approach for remote sensing image classification", *IEEE Transactions on geoscience and remote sensing,* Vol. 56, No. 8, pp. 4420-4434, 2018.

[28] K. Murali, T. H. Sarma, and C. S. Bindu, "A 3D-deep CNN based feature extraction and hyperspectral image classification.", *In 2020 IEEE India Geoscience and Remote Sensing Symposium (InGARSS), IEEE,* pp. 229-232, 2020.

[29] Roy, S. Kumar, G. Krishna, S. R. Dubey, and B. Chaudhuri, "HybridSN: Exploring 3-D–2-D CNN feature hierarchy for hyperspectral image classification.", *IEEE Geoscience and Remote Sensing Letters,* Vol. 17, No. 2, pp. 277-281, 2019.

[30] B. Raviteja, M. S. P. Babu, K. V. Rao, and J. Harikiran, "A New Methodology of Hierarchical Image Fusion in Framework for Hyperspectral Image Segmentation," *Indonesian Journal of Electrical Engineering and Computer Science*, Vol. 6, No. 1, pp. 58-65, 2017.

[31] S. Wan, C. Gong, P. Zhong, B. Du, L. Zhang, and J. Yang, "Multiscale Dynamic Graph Convolutional Network for Hyperspectral Image Classification.", *IEEE Transactions on*

Geoscience and Remote Sensing, Vol. 58, No. 5, pp. 3162-3177, 2020.

[32] Z. Meng, L. Li, L. Jiao, Z. Feng, X. Tang, and M. Liang, "Fully dense multiscale fusion network for hyperspectral image classification.", *Remote Sensing*, Vol. 11, No. 22, 2019.

[33] Mohan and M. Venkatesan, "HybridCNN based hyperspectral image classification using multiscale spatiospectral features", *Infrared Physics & Technology*, Vol. 108, 2020.

[34] M. Kanthi, T. H. Sarma, and C. S. Bindu, "Multi-scale 3D-convolutional neural network for hyperspectral image classification.", *Indonesian Journal of Electrical Engineering and Computer Science*, Vol. 25, No. 1, pp. 307-316, 2022.

[35] B. Alotaibi, and M. Alotaibi, "A Hybrid Deep ResNet and Inception Model for Hyperspectral Image Classification", *PFG–Journal of Photogrammetry, Remote Sensing and Geoinformation Science*, Vol. 88, No. 6, pp. 463-476, 2020.

[36] H. Zhang, Y. Liu, B. Fang, Y. Li, L. Liu, and I. Reid, "Hyperspectral Classification Based on 3D Asymmetric Inception Network with Data Fusion Transfer Learning", arXiv preprint arXiv:2002.04227, 2020.

[37] X. Yang, X. Zhang, Y. Ye, R. Y. K Lau, S. Lu, X. Li, and X. Huang "Synergistic 2D/3D convolutional neural network for hyperspectral image classification", Remote Sensing, Vol. 12, No. 12, pp. 2033, 2020.

[38] Kanthi, Murali, T. Hitendra Sarma, and C. Shoba Bindu. "A 3D-Inception CNN for Hyperspectral Image Classification.", *International Journal of Intelligent Engineering and Systems*, vol.15, no.1, 2022.

[39] J. Ma, and J. Zhao, "Robust topological navigation via convolutional neural network feature and sharpness measure", IEEE Access, Vol. 5, pp. 20707-20715, 2017.